Malignant Fibrous Histiocytoma of the Head and Neck: CT and MR Imaging Findings

S.-W. Park, H.-J. Kim, J.H. Lee and Y.-H. Ko

AJNR Am J Neuroradiol 2009, 30 (1) 71-76
doi: https://doi.org/10.3174/ajnr.A1317
http://www.ajnr.org/content/30/1/71

ORIGINAL RESEARCH

Malignant Fibrous Histiocytoma of the Head and Neck: CT and MR Imaging Findings

S.-W. Park
H.-J. Kim
J.H. Lee
Y.-H. Ko

BACKGROUND AND PURPOSE: Malignant fibrous histiocytoma (MFH) is uncommon in the head and neck. The purpose of this study was to investigate CT and MR imaging features of 13 cases of MFH of this area.

MATERIALS AND METHODS: Two head and neck radiologists, in consensus, retrospectively reviewed CT ($n = 11$) and MR ($n = 9$) images in 13 patients (9 men and 4 women; mean age, 45 years) with histologically proved MFH of the head and neck, paying attention to the location and extent, size, margin, internal architecture, and pattern and degree of enhancement of the lesion. We also investigated if there were any differences in signal-intensity characteristics on MR images, according to different histologic subtypes.

RESULTS: All lesions were seen as well-defined ($n = 2$) or ill-defined ($n = 11$), aggressive masses with a mean size of 4.9 cm. The tumors were primarily located in the sinonasal cavity in 6, the soft tissue of the face and neck in 5, the oral cavity in 1, and the orbital roof in 1. One lesion arose in the bones with background fibrous dysplasia. Twelve lesions invaded the adjacent soft tissues, and bone destruction was seen in 11 lesions. The attenuation, signal intensity, and enhancement pattern of the lesions were nonspecific except for those of myxoid MFH.

CONCLUSIONS: Although rare, MFH of the head and neck is an aggressive tumor that arises most commonly in the sinonasal tract and is frequently associated with soft-tissue invasion and bone destruction on CT and MR images.

Malignant fibrous histiocytoma (MFH) is the most common soft-tissue sarcoma in adults, accounting for 20%–30% of all soft-tissue sarcomas.[1-3] It was first recognized as a distinct clinicopathologic entity in the early 1960s as a pleomorphic sarcoma that contains both fibroblastic and histiocytic cells in varying proportions, arranged in a storiform pattern.[4-6] In addition to soft tissue, the tumor has been reported to occur in virtually every part of the body, including bone, viscera, and skin.[2,7] Despite this ubiquity, however, MFH remains relatively uncommon in the head and neck region, accounting for 3%–10% of all cases.[8,9] To our knowledge, except in a limited number of case reports,[10-13] most of the previous reports on MFH of the head and neck focused on the clinicopathologic features,[8,9,14-16] and the imaging features were not the major concern. The purpose of this study was to investigate the CT and MR imaging features of 13 cases of MFH arising in various locations of the head and neck.

Materials and Methods

Patients

The institutional review board approved this retrospective study.

We reviewed CT ($n = 11$) and MR ($n = 9$) images obtained from 13 patients with histologically proved MFH in the head and neck. The patients were recruited after a review of medical records from 3 tertiary referral academic centers during the past 10 years. There were 9 men and 4 women, 24–65 years of age, with a mean age of 45 years. Seven patients underwent both CT and MR imaging examinations.

Ten patients presented with a palpable mass or swelling of the face and neck, and 3 patients, with nasal obstruction, which had first been noticed 1 month to 3 years before (mean, 4.5 months). Three patients also had pain. All patients denied a history of previous irradiation, trauma, or surgery at the tumor sites. The histologic subtype could be established in 12 of 13 tumors, including 7 storiform-pleomorphic types, 2 myxoid types, 2 inflammatory types, and 1 mixed form of storiform-pleomorphic and myxoid types.

Imaging Techniques

CT scanning was performed in 11 patients, and MR imaging, in 9 patients. Seven patients underwent both CT and MR imaging examinations. CT scans were obtained in the axial plane by using various models of a helical CT scanner with 2.5- to 3.75-mm section thicknesses. In 9 patients, CT scans after the intravenous administration of iodinated contrast material were available for review; of these 9, precontrast CT scans were also available in 6. In the remaining 2 patients, CT scans were obtained without the use of contrast material.

MR imaging examinations were performed on a 1.5T ($n = 8$; Signa Advantage, GE Healthcare, Milwaukee, Wis) or a 3T ($n = 1$; Intera Achieva, Philips Medical Systems, Best, the Netherlands) scanner by using a head or neurovascular coil. In all patients, precontrast T1-weighted spin-echo images (TR/TE/NEX, 400–560 ms/10–14 ms/2) and T2-weighted fast spin-echo images (TR/TE/NEX, 2500–4500 ms/80–110 ms/1) with or without fat saturation were obtained, followed by contrast-enhanced T1-weighted spin-echo images with or without fat saturation after the intravenous injection of 0.1 mmol/kg of gadopentetate dimeglumine. Images were obtained in at least 2 planes with 3- to 4-mm section thickness, 0- to 0.4-mm intersection gap, 256 × 192 matrix, and 22-cm FOV.

Image Analysis

Two experienced head and neck radiologists (with clinical experience of 18 and 9 years) retrospectively reviewed all of the CT and MR

Received June 3, 2008; accepted after revision August 10.

From the Department of Radiology (S.-W.P.), Inha University College of Medicine, Incheon, Korea; Departments of Radiology (H.-J.K.) and Pathology (Y.-H.K.), Samsung Medical Center, Sungkyunkwan University School of Medicine, Seoul, Korea; and Department of Radiology and Research Institute of Radiology (J.H.L.), University of Ulsan College of Medicine, Asan Medical Center, Seoul, Korea.

Please address correspondence to Hyung-Jin Kim, MD, Department of Radiology, Samsung Medical Center, Sungkyunkwan University School of Medicine, 50 Ilwon-Dong, Kangnam-Ku, Seoul, Korea; e-mail: hyungkim@skku.edu

DOI 10.3174/ajnr.A1317

images for consensus. We investigated the CT and MR imaging characteristics with emphasis on the location and extent, size, margin, internal architecture, and pattern and degree of enhancement of the lesion. The size of the lesion was measured at its greatest diameter. The margin of the lesion was classified as well-defined and ill-defined. As for internal architecture, we compared the attenuation of the lesion on precontrast CT scans with that of the adjacent muscle. The signal intensity of the lesion on T1- and T2-weighted MR images was compared with that of the cerebral cortex. The presence of any calcification within the lesion determined on precontrast CT scans was also recorded. On postcontrast CT and MR images, the pattern of enhancement at the solid portions of the lesion was categorized as homogeneous or heterogeneous. The degree of enhancement was subjectively assessed as being mild, moderate, and marked. We also investigated any differences in signal-intensity characteristics on MR images according to the different histologic subtypes.

Results

The CT and MR imaging features of 13 cases of MFH of the head and neck are summarized in the Table. All lesions were seen as well-defined ($n = 2$) or ill-defined ($n = 11$) aggressive soft-tissue masses in various locations of the head and neck, ranging in size from 2.5 to 7.8 cm (mean, 4.9 cm). The centers of the lesions appeared to be the sinonasal tract in 6 cases (46%), including the maxillary sinus ($n = 4$; Fig 1) and the nasal cavity ($n = 2$); the soft tissue of the face and neck in 5 cases (38%), including the masticator space ($n = 2$; Fig 2), the anterior cheek ($n = 1$; Fig 3), the infraparotid lateral neck ($n = 1$), and the poststyloid parapharyngeal space ($n = 1$); and the oral cavity involving the upper anterior gingiva in 1 case (8%). The remaining lesion (8%) was thought to arise from the orbital roof (Fig 4). In this case, there was radiographic evidence of fibrous dysplasia in the background cranial bones on CT and MR images. All of the lesions, except 1 in the oral cavity, invaded the adjacent soft tissues of the face and neck, 1 of which also extended into the intracranial cavity. Eleven lesions including all of 6 sinonasal lesions and 1 orbital roof lesion were accompanied by bone destruction.

Compared with the adjacent muscle, the attenuation of the lesion seen on precontrast CT scans obtained in 8 patients was isoattenuated in 4, hypoattenuated in 2, and mixed isoattenuated and hypoattenuated in 2. There was 1 case showing intratumoral calcifications on precontrast CT scans (Fig 2*A*). Compared with the cerebral cortex, the signal intensity of 9 lesions examined by MR imaging varied as homogeneous isointensity in 4, heterogeneous isointensity with hyper- and/or hypointensity in 4, and homogeneous hypointensity in 1 on T1-weighted images. T2-weighted images showed heterogeneous isointensity with hyper- and/or hypointensity in 7 and homogeneous hyperintensity in 2. On postcontrast CT and MR images, there was homogeneous ($n = 2$) or heterogeneous ($n = 7$) moderate-to-marked enhancement in 9 and heterogeneous mild-to-moderate enhancement in 4 at the solid portion of the lesions. Various portions of no enhancement, probably representing intratumoral necrosis or hemorrhage, were found in 11 lesions.

Of the 12 lesions whose histologic subtypes could be classified, MR imaging was performed in 8, including 5 storiform-pleomorphic types, 2 inflammatory types, and 1 myxoid type. Except for the myxoid type, which demonstrated homogeneous marked hyperintensity on T2-weighted images and homogeneous marked enhancement on contrast-enhanced images (Fig 3), there was little difference in signal-intensity characteristics between the storiform-pleomorphic and inflammatory types on MR images.

Discussion

The term "MFH" or "pleomorphic sarcoma" was first introduced in the early 1960s to refer to a group of soft-tissue tumors, characterized by a storiform or cartwheel-like growth pattern.[2,4-6] The histogenesis of this tumor still remains controversial. Once thought of as a tumor of a histiocytic origin, recent advances of immunohistochemistry and numerous monoclonal antibodies demonstrated a closer phenotypic link with the fibroblasts, myofibroblasts, or undifferentiated mesenchymal cells.[2,3] Because of common complex nonuniform cytogenetic aberrations as well as the pleomorphic nature of the tumor, many lesions diagnosed as MFH might eventually prove to be lineage-specific sarcomas, and the reported incidence of the tumors that remain unclassified even after rigorous evaluation has been 20%–70%.[2,17]

Histopathologically, MFH can be divided into the following 4 morphologic subtypes in decreasing order, depending on the predominant cellular components: storiform-pleomorphic (50%–60%), myxoid (25%), giant cell (5%–10%), and inflammatory (< 5%), some of which have prognostic significance.[2,3,12,18] The myxoid variant has better prognosis compared with the storiform-pleomorphic type. It is not unusual for several morphologic patterns to be observed within 1 lesion.[12]

Clinically, patients with MFH usually present with an enlarging, painless, solid soft-tissue mass, most frequently in the lower extremity followed by the upper extremity and the retroperitoneum.[2,3] Most patients are between 50 and 70 years of age, and men are affected 2–3 times as commonly as women. Retroperitoneal tumors are often larger than extremity lesions, whereas subcutaneous tumors are smaller.[2,3] Wide local excision with negative margins is considered the treatment of choice for MFH. Postoperative radiation therapy is reported to improve local control. The overall 5-year survival rate of MFH has been reported to be 58%–77%.[16,19,20] Tumor grade, size, depth, histologic subtype, and distant metastases at initial presentation seem to be the important prognostic factors for MFH.[2,19] The tumor has a local recurrence rate of 19%–31% and a metastatic rate of 31%–35%. The common metastatic sites are the lung (90%), bone (8%), and liver (1%).[2] The incidence of regional lymph node metastasis is relatively low, varying between 4% and 17%.[2]

The head and neck region is an uncommon site for MFH, where 3%–10% of all MFHs occur.[8,9] In the head and neck, MFH has been reported to involve the nasal cavity and paranasal sinuses most frequently, accounting for 30% of all cases.[8,9,16] Of the sinonasal tract, it occurs most commonly in the maxillary sinus, followed by the ethmoid sinus, nasal cavity, sphenoid sinus, and frontal sinus.[9] Other reported sites involved in the head and neck include the craniofacial bones (15%–25%), larynx (10%–15%), soft tissue of the neck (10%–15%), major salivary gland (5%–15%), oral cavity (5%–15%), pharynx, ear, and eyelid.[8,9,13] As in the extremities, the sto-

Summary of CT and MR imaging features of 13 patients with MFH of the head and neck*

Patient No./ Age(yr)/Sex	CT/MR Image	Center/Extent	BD	Size (cm)	Margin	Density on Precontrast CT	T1WI	T2WI	Enhancement Pattern/Degree	Histologic Subtype
1/65/F	No/yes	Maxillary sinus/nasal cavity, orbit, buccal space, anterior cheek	Yes	5.5	Ill-defined	–	Mixed isointense, hypointense	Mixed isointense, hyperintense, hypointense	Heterogeneous/moderate	Inflammatory
2/46/F	Yes/yes	Maxillary sinus/buccal space	Yes	4.0	Ill-defined	Isodense	Mixed isointense, hyperintense	Mixed isointense, hyperintense, hypointense	Heterogeneous/moderate	Inflammatory
3/42/M	Yes/no	Nasal cavity/maxillary sinus, ethmoid sinus, buccal space	Yes	5.0	Ill-defined	Mixed isodense, slightly hypodense	–	–	Heterogeneous/mild to moderate	Myxoid
4/58/M	Yes/no	Maxillary sinus/anterior cheek	Yes	3.9	Ill-defined	Mixed isodense, slightly hypodense	–	–	Heterogeneous/moderate	Storiform-pleomorphic
5/34/M	Yes/yes	Maxillary sinus/nasal cavity, ethmoid sinus, orbit, buccal space, anterior cheek	Yes	4.0	Ill-defined	Isodense	Mixed isointense, hyperintense, hypointense	Mixed hyperintense, isointense, hypointense	Heterogeneous/moderate	Storiform-pleomorphic
6/46/M	Yes/yes	Nasal cavity/nasopharynx, nasal septum	Yes	4.1	Ill-defined	–	Isointense	Mixed isointense, hypointense	Heterogeneous/moderate	Storiform-pleomorphic
7/57/M	Yes/yes	Masticator space/zygomatic arch	Yes	7.8	Ill-defined	Isodense	Isointense	Mixed isointense and hyperintense	Heterogenous/marked	–
8/30/M	Yes/yes	Masticator space/zygomatic arch, middle cranial base, middle cranial fossa	Yes	5.8	Ill-defined	Isodense	Mixed isointense and hyperintense	Mixed isointense and hyperintense	Heterogeneous/moderate to marked	Storiform-pleomorphic
9/39/M	Yes/yes	Anterior cheek/nasal cavity, frontal process of maxilla	Yes	4.5	Well-defined	Slightly hypodense	Slightly hypointense	Markedly hyperintense	Homogeneous/marked	Myxoid
10/24/M	Yes/no	Infraparotid lateral neck/ sternocleidomastoid muscle, parotid gland	No	6.8	Ill-defined	–	–	–	Heterogeneous/mild to moderate	Mixed storiform-pleomorphic and myxoid
11/60/M	Yes/no	Poststyloid parapharyngeal space/prevertebral space/ carotid artery	No	5.2	Ill-defined	–	–	–	Heterogeneous/mild to moderate	Storiform-pleomorphic
12/41/F	No/yes	Upper anterior gingiva/maxillary alveolar bone	Yes	2.5	Well-defined	–	Isointense	Hyperintense	Homogeneous/moderate	Storiform-pleomorphic
13/45/F	Yes/yes	Orbital roof/orbit, facial soft tissue	Yes	5.0	Ill-defined	Hypodense	Isointense	Mixed isointense and hyperintense	Heterogenous/mild to moderate	Storiform-pleomorphic

Note:—BD indicates associated bone destruction; T1WI, T1-weighted imaging; T2WI, T2-weighted imaging; MFH, malignant fibrous histiocytoma.
* Size was denoted as greatest diameter; density of the lesion was compared with that of the adjacent muscle; signal intensity of the lesion was compared with that of the cerebral cortex.

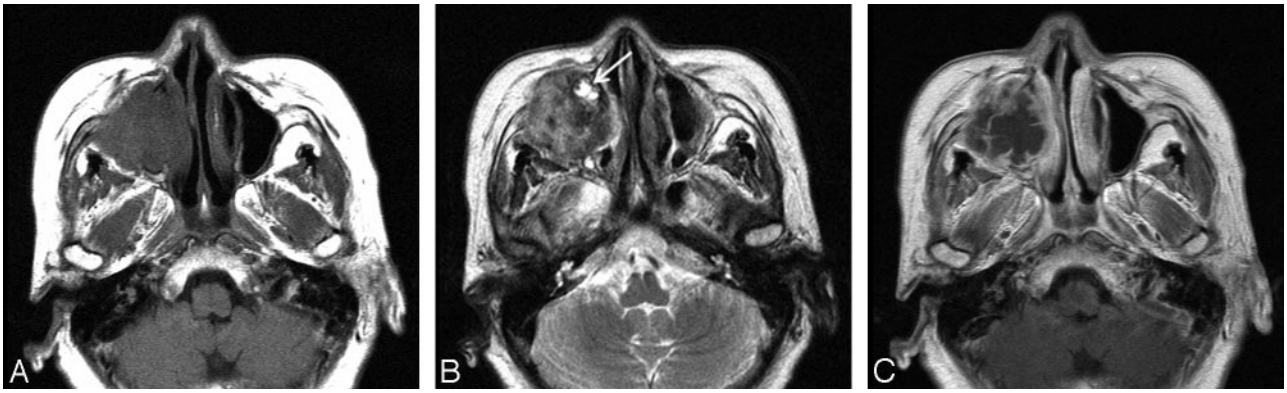

Fig 1. Case 1. Inflammatory type of MFH of the maxillary sinus in a 65-year-old woman. Axial MR images show a large ill-defined mass in the right maxillary sinus, which causes destruction of the sinus walls, extending into the anterior cheek and retromaxillary fat. *A* and *B*, Compared with the adjacent muscle, the signal intensity of the mass is mixed isointense and slightly hypointense on the T1-weighted image (*A*) and mixed hyperintense, isointense, and hypointense on the T2-weighted image (*B*). *C*, On the contrast-enhanced T1-weighted image, there is moderate heterogeneous enhancement at the periphery of the mass with the central areas remaining unenhanced. Also note that the mass invades the nasolacrimal duct, which is enlarged and filled with fluid (*arrow* in *B*).

Fig 2. Case 7. MFH of the lateral cheek in a 57-year-old man. *A*, Precontrast axial CT scan shows a large ill-defined soft-tissue mass involving the left masticator space with extension to the skin. The mass is isoattenuated to the adjacent muscle and contains several coarse and irregular calcifications peripherally (*arrows*). Postcontrast CT scans demonstrated marked heterogeneous enhancement within the mass (data not shown). *B*, Compared with the cerebral cortex, the signal intensity of the mass is mixed isointense and hyperintense on the axial fat-suppressed T2-weighted MR image. T1-weighted images demonstrated homogeneous isointense signal intensity of the mass (data not shown). *C*, On the contrast-enhanced axial fat-suppressed T1-weighted MR image, there is marked heterogeneous enhancement within the mass. Also note the involvement of the zygoma by the mass (*arrows*).

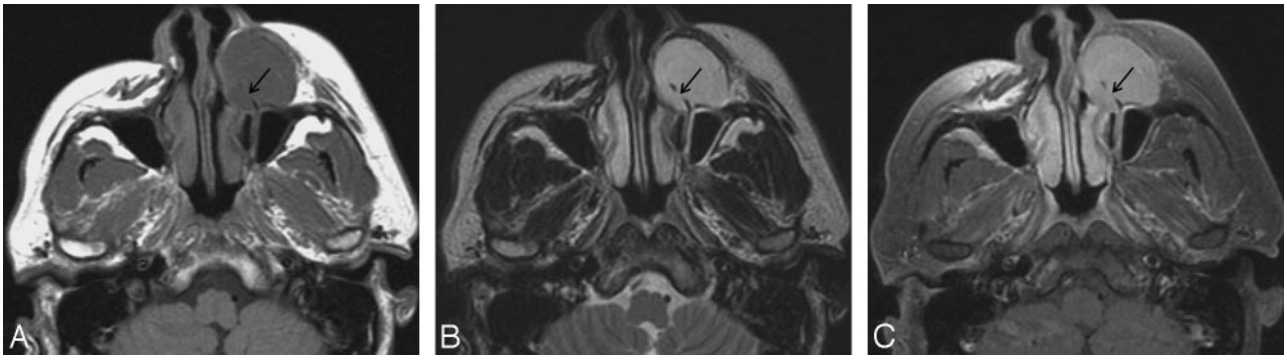

Fig 3. Case 9. Myxoid type of MFH of the anterior cheek in a 39-year-old man. Axial MR images show a well-defined ovoid soft-tissue mass in the left anterior cheek. The mass causes erosion of the frontal process of the maxilla (*arrows*). *A* and *B*, Compared with the cerebral cortex, the signal intensity of the mass is slightly hypointense on the T1-weighted image (*A*) and markedly hyperintense on the T2-weighted image (*B*). *C*, Contrast-enhanced fat-suppressed T1-weighted image shows marked homogeneous enhancement throughout the mass.

riform-pleomorphic type is the most common subtype, followed by the myxoid type.[16]

In general, head and neck MFH is reported to be associated with a poorer prognosis, compared with MFH elsewhere in the body. It poses a great challenge to surgeons due to the anatomic and functional complexity of the head and neck. Inadequate removal of the tumor is associated with a high recurrence rate of 20%–42%. Systemic metastases are also common, reported in 25%–35%.[8,9] Recently, Sabesan et al[16] reported a 48% 5-year survival rate for MFH of the head and neck, which is much lower than 77% for MFH of the trunk and extremities. Tumors that extend into bony structures are associated with a much more aggressive clinical course than those that are restricted to soft tissues.[15] Because the reported frequency of nodal metastases for head and neck MFH varies between 0% and 15%, elective neck dissection is usually not

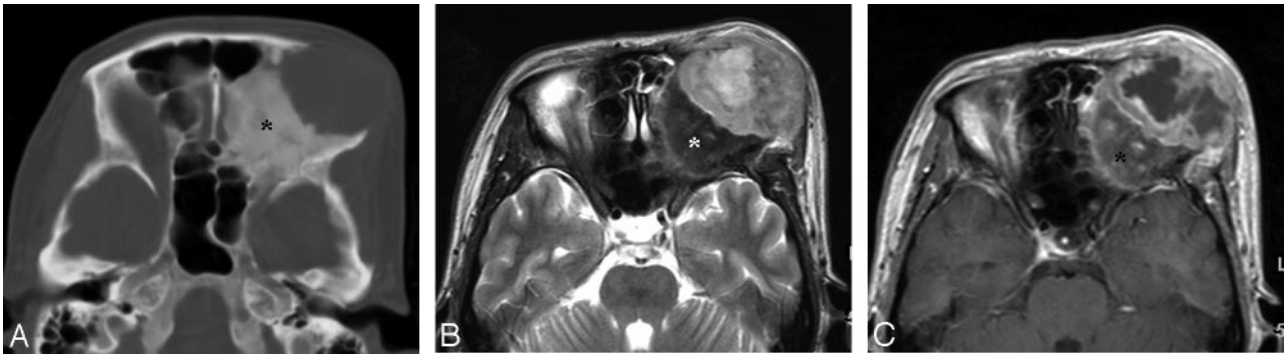

Fig 4. Case 13. Storiform-pleomorphic type of MFH of the orbital roof secondary to fibrous dysplasia in a 45-year-old woman. *A*, Postcontrast axial CT scan with bone window setting shows a large ill-defined osteolytic lesion in the left orbital roof. The adjacent cranial bones demonstrate a diffuse ground-glass appearance, typical of fibrous dysplasia (*asterisk*). *B* and *C*, On the axial MR images, the lesion is seen as a large ill-defined mass extending to the anterior face. Compared with the adjacent muscle, the signal intensity of the mass is mixed isointense and hyperintense on the T2-weighted image (*B*). T1-weighted images demonstrated isointense signal intensity of the mass (data not shown). On the contrast-enhanced T1-weighted image (*C*), there is mild-to-moderate heterogeneous enhancement at the periphery of the mass with the central areas remaining unenhanced. The background bone with fibrous dysplasia is markedly hypointense on the T2-weighted image and enhances heterogeneously after administration of contrast material (*asterisks*).

performed; it is performed only when there is clinical, histologic, or radiologic evidence of metastases.[8,9,15]

The results of our study are in accord with those of others. The sinonasal tract was the most common site of origin (46% in our study), followed by the soft tissue of the face and neck (38%), the oral cavity (8%), and the craniofacial bones (8%). The occurrence was primarily in middle-aged adults (mean, 45 years) with men affected more frequently than women (9:4). Our study also revealed that MFH of the head and neck is an aggressive neoplasm with frequent soft-tissue invasion ($n = 12$) and bone destruction ($n = 11$). There was no evidence of perineural tumor spread on the imaging studies.

Although the imaging studies were very helpful for surgical planning by adequate demonstration of the tumor extent, the specific radiologic diagnosis was difficult to make because most of the tumors in this study showed nonspecific varying-attenuation, signal intensity, and enhancement on CT and MR images. The reported CT and MR imaging features of MFH have also been nonspecific.[3,18,21-23] On CT scans, MFH is usually seen as a large lobulated soft-tissue mass, which is isoattenuated to muscle. Calcification or ossification can be detected in 5%–20%. The center of the lesion often has diminished attenuation due to necrosis, hemorrhage, or myxoid material.[3,18,22] On MR images, MFH is typically seen as a mass that is isointense to muscle on T1-weighted images and heterogeneously hyperintense on T2-weighted images.[3,18,21-23]

MR images often show heterogeneous signal intensity on all pulse sequences, reflecting the complex histologic components of the tumor. This histologic complexity can be displayed best on T2-weighted images; whereas the areas of abundant fibrous tissue appear hypointense, those of abundant myxoid stroma appear hyperintense.[3,21] Spontaneous hemorrhage is not infrequent. It is occasionally accompanied by fluid-fluid levels, and is seen as areas of time-dependent varying signal intensity on MR images. Sometimes those hemorrhagic areas are so extensive as to obscure the underlying neoplasm.[3,21] Variable heterogeneous enhancement of solid components of the tumor, usually nodular and peripheral, is seen on contrast-enhanced CT and MR images.[3,18]

In general, the signal-intensity characteristics of MR imaging according to various histologic subtypes were not different in our study. However, the myxoid type demonstrated rather characteristic signal intensity on MR images—that is, homogeneous marked hyperintensity on T2-weighted images and homogeneous marked enhancement on contrast-enhanced images (Fig 3). Myxoid MFH is usually seen as a mass with signal intensity similar to that of fluid on T1- and T2-weighted images due to the high water content.[3] After administration of contrast material, there is often nodular and peripheral enhancement of the nonmyxomatous more cellular regions.[3,22] Sometimes, as in our cases, the myxoid tissue is more vascular and shows a higher degree of cellularity, resulting in a more homogeneous soft-tissue mass with diffuse contrast enhancement on MR images.[3] Other soft-tissue neoplasms with a myxoid appearance include myxoid liposarcoma, myxoid chondrosarcoma, myxoid leiomyosarcoma, neurogenic tumor, and myxoma.[3,22]

Most interesting in our study, 1 case of MFH demonstrated radiographic evidence of fibrous dysplasia in the background cranial bones. Although rare, fibrous dysplasia is known for the potential for malignant change, with the estimated frequency of 0.5% for monostotic type and 4% for McCune-Albright syndrome.[24] The associated sarcomas include osteosarcoma, fibrosarcoma, chondrosarcoma, and MFH. Early diagnosis of an associated malignancy with cross-sectional imaging gives a better chance for a cure.[24] MFH has also been reported to occur secondary to irradiation, trauma, Paget disease, osteonecrosis, chronic osteomyelitis, and benign bone tumors such as enchondroma and giant cell tumor.[10,22,23,25] Compared with the tumors that arise de novo, secondary MFHs are reported to be more aggressive with a poorer prognosis.[8,22,24]

Head and neck MFH can be confused with a variety of fibrous tumors and inflammatory conditions, including neurilemmoma, fibromatosis, premature sarcoma, hemangiopericytoma, granuloma, nodular fasciitis, malignant mesenchymal tumor, myoblastoma, fat necrosis, Langerhans cell histiocytosis, pleomorphic rhabdomyosarcoma, and fibrosarcoma.[14]

Conclusions

Although rare, MFH is an aggressive tumor that arises in various locations of the head and neck, most commonly the sinonasal tract. It is frequently associated with soft-tissue inva-

sion and bone destruction on CT and MR images. Although the imaging findings are rather nonspecific, CT and MR imaging studies are essential for preoperative staging and surgical planning in patients with MFH of the head and neck.

References

1. Weiss SW, Enzinger FM. **Malignant fibrous histiocytoma: an analysis of 200 cases.** *Cancer* 1978;41:2250–66
2. Weiss SW, Goldblum JR. *Enzinger and Weiss's Soft Tissue Tumors.* 5th ed. St. Louis: Mosby; 2008:403–27
3. Kransdorf M, Murphey M. *Imaging of Soft Tissue Tumors***.** Philadelphia: Lippincott Williams & Wilkins; 2006:257–97
4. Kauffman SL, Stout AP. **Histiocytic tumors (fibrous xanthoma and histiocytoma) in children.** *Cancer* 1961;14:469–82
5. Ozzello L, Stout AP, Murray MR. **Cultural characteristics of malignant histiocytomas and fibrous xanthomas.** *Cancer* 1963;16:331–44
6. O'Brien JE, Stout AP. **Malignant fibrous xanthomas.** *Cancer* 1964;17:1445–55
7. Huvos AG, Heilweil M, Bretsky SS. **The pathology of malignant fibrous histiocytoma of bone: a study of 130 patients.** *Am J Surg Pathol* 1985;9:853–71
8. Barnes L, Kanbour A. **Malignant fibrous histiocytoma of the head and neck: a report of 12 cases.** *Arch Otolaryngol Head Neck Surg* 1988;114:1149–56
9. Rodrigo JP, Fernandez JA, Suarez C, et al. **Malignant fibrous histiocytoma of the nasal cavity and paranasal sinuses.** *Am J Rhinol* 2000;14:427–31
10. Nakayama K, Nemoto Y, Inoue Y, et al. **Malignant fibrous histiocytoma of the temporal bone with endocranial extension.** *AJNR Am J Neuroradiol* 1997;18:331–34
11. Lakhani P, Rubesin SE, Zhang PJ. **Malignant fibrous histiocytoma of the pharynx.** *AJR Am J Roentgenol* 2005;184:S12–S13
12. Senel FC, Bektas D, Caylan R, et al. **Malignant fibrous histiocytoma of the mandible.** *Dentomaxillofac Radiol* 2006;35:125–28
13. Nagano H, Deguchi K, Kurono Y. **Malignant fibrous histiocytoma of the bucca: a case report.** *Auris Nasus Larynx* 2008;35:165–69
14. Sawyer R, Webb DL, Wittich DJ. **Head and neck malignant fibrous histiocytomas.** *Ear Nose Throat J* 1993;72:299–302
15. Iguchi Y, Takahashi H, Yao K, et al. **Malignant fibrous histiocytoma of the nasal cavity and paranasal sinuses: review of the last 30 years.** *Acta Otolaryngol Suppl* 2002;547:75–78
16. Sabesan T, Xuexi W, Yongfa Q, et al. **Malignant fibrous histiocytoma: outcome of tumors in the head and neck compared with those in the trunk and extremities.** *Br J Oral Maxillofac Surg* 2006;44:209–12
17. Engellau J, Anerson H, Rydholm A, et al. **Time dependence of prognostic factors for patients with soft tissue sarcomas: a Scandinavian Group Study of 338 malignant fibrous histiocytomas.** *Cancer* 2004;100:2233–39
18. Munk PL, Sallomi DF, Janzen DL, et al. **Malignant fibrous histiocytoma of soft tissue imaging with emphasis on MRI.** *J Comput Assist Tomogr* 1998;22:819–26
19. Gibbs JF, Huang PP, Lee RJ, et al. **Malignant fibrous histiocytoma: an institutional review.** *Cancer Invest* 2001;19:23–27
20. Hsu HC, Huang EY, Wang CJ. **Treatment results and prognostic factors in patients with malignant fibrous histiocytoma.** *Acta Oncol* 2004;43:530–35
21. Mahajan H, Kim EE, Wallace S, et al. **Magnetic resonance imaging of malignant fibrous histiocytoma.** *Magn Reson Imaging* 1989;7:283–88
22. Murphey M, Gross T, Rosenthal H. **Musculoskeletal malignant fibrous histiocytoma: radiologic-pathologic correlation.** *Radiographics* 1994;14:807–26
23. Link TM, Haeussler MD, Poppek S, et al. **Malignant fibrous histiocytoma of bones: conventional x-ray and MR imaging features.** *Skeletal Radiol* 1998;27:552–58
24. Hoshi M, Matsumoto S, Manabe J, et al. **Malignant change secondary to fibrous dysplasia.** *Int J Clin Oncol* 2006;11:229–35
25. Makimoto Y, Yamamoto S, Takano H, et al. **Imaging findings of radiation-induced sarcoma of the head and neck.** *Br J Radiol* 2007;80:790–97